AAPS PharmSciTech (2026) 27:148
https://doi.org/10.1208/s12249-026-03351-4

RESEARCH ARTICLE

Engineered Lecithin-Polymer Hybrid Micelles for Enhanced Gallic Acid Delivery: Response Surface Optimization and Preclinical Evaluation

Nabila M. Sweed[1] · **Mahitab H. Elbishbishy**[2] · **Mai A. Zaafan**[3]

Received: 4 November 2025 / Accepted: 16 January 2026

Abstract

Oxidative stress is regarded as a major pathogenic key factor in chronic idiopathic pulmonary fibrosis (IPF), a disease with high mortality and an unclear cause. Gallic acid (GA) is a natural polyphenolic compound that shows significant antioxidant potential. However, its therapeutic effectiveness is limited due to low oral bioavailability, rapid metabolism, and poor aqueous solubility. To overcome such barriers, lecithin–polymer hybrid micelles (LPHM) were engineered as a nanocarrier platform for GA delivery. This study investigated the formulation and optimization of GA-loaded LPHM for pulmonary fibrosis therapy. LPHM were optimized using a D-optimal experimental design, assessing the drug amount (X_1) and polymer type (X_2: Pluronic® P123 or D-α-tocopheryl polyethylene glycol succinate, TPGS) on entrapment efficiency (Y_1), particle size (Y_2), and zeta potential (Y_3). The optimized formula, comprising TPGS with 17 mg GA, showed an entrapment efficiency of 96.78 ± 1.45%, a particle size of 120.22 ± 1.45 nm, and a zeta potential of − 32.12 ± 0.97 mV. *In-vitro* release demonstrated a biphasic sustained-release profile. *In-vivo* pharmacokinetics showed a 7.35-fold increase in oral bioavailability of the optimized formula as compared to free GA. In a bleomycin-induced IPF model, the optimized formula significantly mitigated fibrotic progression, as evidenced by reductions in transforming growth factor-β, matrix metalloproteinase-7, hydroxyproline, and collagen-1. Overall, GA-loaded LPHM represent a promising oral drug delivery strategy for IPF, with broader potential in managing chronic diseases that demand sustained release and enhanced systemic exposure.

Keywords gallic acid · lecithin-based micelles · pulmonary fibrosis · pluronics

Introduction

Idiopathic pulmonary fibrosis (IPF) is an ultimately lethal interstitial lung disorder marked by remodelling of the airways, inflammatory responses and widespread fibrotic changes in the lung parenchyma. Without a lung transplant, median survival following diagnosis is only 3 to 5 years, a prognosis comparable to that of many aggressive malignancies [1–4]. Despite FDA approval of pirfenidone and nintedanib in 2014, these drugs fail to significantly reduce mortality and are often limited by adverse effects such as gastrointestinal disturbances, underscoring the urgent need for more effective and better tolerated therapies [5].

Although the exact etiology of IPF is still unknown, it is generally accepted that oxidative stress, persistent inflammation, and an abnormal accumulation of extracellular matrix are important factors in the development of such disorder. Reactive oxygen species (ROS) causes pulmonary tissue death and activates fibroblasts and immune cells, perpetuating fibrotic remodelling [6–8]. Accordingly, antioxidant-based strategies have gained attention as potential therapeutic interventions thus may benefit IPF patients.

Among natural antioxidants, phenolic compounds are particularly promising owing to their dual mechanisms: direct scavenging of free radicals and modulation of cellular signalling to upregulate endogenous antioxidant defences [9, 10].

Gallic acid (GA), a trihydroxy benzoic acid derivative, has demonstrated potent antioxidant activity and protective effects against oxidative stress [11–13]. However, its

✉ Nabila M. Sweed
nabila.msweed@gmail.com; nsueed@msa.edu.eg

[1] Department of Pharmaceutics, Faculty of Pharmacy, October University for Modern Sciences and Arts, Giza, Egypt

[2] Department of Pharmacognosy, Faculty of Pharmacy, October University for Modern Sciences and Arts, Giza, Egypt

[3] Department of Pharmacology, Faculty of Pharmacy, October University for Modern Sciences and Arts, Giza, Egypt

Published online: 18 March 2026

therapeutic translation is hindered by poor aqueous solubility, suboptimal absorption, and rapid metabolism, resulting in poor systemic bioavailability [14].

The self-assembly of amphiphilic block copolymers produces polymeric micelles (PMs) which have a hydrophilic shell that improves systemic stability and prolongs circulation time in addition to a hydrophobic core that increases the solubility of medications with low water solubility. Having nanoscale dimensions of approximately 10–100 nm, these carriers are capable of prolonging systemic circulation by minimizing the reticuloendothelial system uptake and the kidney filtration [15–18]. Additionally, block copolymers are widely used to inhibit drug efflux, further enhancing therapeutic effectiveness. Likely, D-α-tocopheryl polyethylene glycol 1000 succinate (TPGS) not only solubilizes hydrophobic drugs but also prolongs circulation time and enhances cellular uptake [19–22]. Lecithin, a naturally occurring phospholipid mixture, has been also extensively utilized in nanoparticle formulations owing to its amphiphilicity, biocompatibility, and ability to improve drug solubilization and stability [23]. Incorporating lecithin into polymeric micelles yields LPHM, which integrate the advantages of both lipid and polymeric systems, leading to improved encapsulation efficiency, higher stability, and superior drug loading compared with conventional micelles [24, 25].

Leveraging these advantages, the present study employs a D-optimal experimental design to optimize gallic acid–loaded LPHM. The overarching aim is to improve the solubility, stability, and oral bioavailability of gallic acid, thus enabling the therapeutic use of this LPHM as a new antioxidant-based approach for treating idiopathic pulmonary fibrosis (IPF).

Materials and Methods

Plant Material

One Kg of the dried powdered leaf buds of *Camellia sinensis* L. family Theaceae was purchased from the local Egyptian market, Giza, Egypt.

Chemicals

Phosphatidyl choline (Soybean lecithin) (90% purity), Pluronic® P123 and Vitamin E d-alpha tocopheryl polyethylene glycol 1000 succinate (TPGS), dapagliflozin (the internal standard) were purchased from Sigma–Aldrich (St. Louis, MO, USA). Bleomycin sulphate was obtained from RMPL Pharma LLP., Egypt. All the other chemicals that were used are of analytical grade.

Animals

Albino Male Wistar rats weighing 150–200 grams were used in this study. The rats were kept at the animal facility of October University for Modern Sciences and Arts after being purchased from the Theodor Bilharz Research Institute in Cairo, Egypt. Under well-maintained circumstances, each rat was housed in a ventilated plastic cage with a temperature of 25 ± 3°C and a relative humidity of 50%. The rats were allowed unrestricted access to water and a typical pellet meal throughout the research. The October University for Modern Sciences and Arts Institutional Animal Care and Use Committee (IACUC) examined and approved the research procedure, which complied with national ethical guidelines for the use and care of laboratory animals. (Approval No. PH77/REC77/2025PD).

Methods

Extraction and Isolation of Gallic Acid

The powdered leaf buds were macerated at room temperature in a solvent composed of 95% ethanol in distilled water (1:1) till exhaustion. The dried hydro-ethanolic extracts were combined to yield greenish-brown residue weighing 77.4 g. The dried extract was successively partitioned with hexane, dichloromethane, ethyl acetate, and n-butanol. Then, the ethyl acetate fraction was subjected to column chromatography over polyamide column and was further purified on a Sephadex LH-20 column to yield an off-white amorphous powder (915 mg). Detailed extraction and isolation procedures are described in the supplementary section.

Experimental Design

Using Design Expert® software, a D-optimal experimental design was performed to assess the impact of independent variables on the properties of lecithin–polymer hybrid micelles. (Version 13, Stat-Ease Inc., Minneapolis, MN). The independent factors included the drug amount (mg) (X_1) and the polymer type (X_2), while the dependent factors were entrapment efficiency (EE%) (Y_1), particle size (nm) (Y_2), and zeta potential (mV) (Y_3). According to the D-optimal design, the composition of the 17 prepared formulae, as suggested by Design Expert® software is shown in Table I. In addition to standard metrics, the model's quality was evaluated by using the regression coefficient and adequate precision. ANOVA was used to verify the statistical model significance and to confirm that it adequately represented the data (i.e., demonstrated a non-significant lack of fit) [26]. The optimal formula (O1) was determined through a

Table I D-optimal Design of Gallic Acid-loaded Lecithin-polymer Hybrid Micelles, and the Composition of the 17 Formulae

Factors (Independent Variables)	**Level Used**				
	−1	**1**			
X_1: Drug amount (mg)	**10**	**55**			
X_2: Type of Polymer	TPGS	**Pluronic P123**			
Response (Dependent Variables)	**Constraints**				
Y_1: Entrapment Efficiency (%)	**Maximize**				
Y_2: Particle Size (nm)	**Minimize**				
Y_3: Zeta Potential (mV)	**Maximize**				
Formula Number	**X1: Amount of drug (mg)**	**Type of Polymer**	**Y1: EE%**	**Y2: PS (nm)**	**Y3: ZP (mv)**
1	43.75	TPGS	48 ± 0.45	132.4 ± 0.34	−34.1 ± 0.21
2	43.75	P123	72 ± 0.21	188.1 ± 0.45	−35.5 ± 0.44
3	55	P123	72.27 ± 0.98	179.1 ± 0.13	−35.1 ± 0.27
4	55	TPGS	71.13 ± 1.65	164.2 ± 0.44	−33.3 ± 0.22
5	55	P123	77 ± 0.89	179.2 ± 0.37	−34.6 ± 0.13
6	21.25	P123	82 ± 0.51	198.2 ± 0.16	−36.3 ± 0.27
7	10	P123	66.15 ± 0.67	192.2 ± 0.22	−39.1 ± 0.11
8	32.5	P123	57 ± 0.54	147.1 ± 0.41	−37.1 ± 0.23
9	10	P123	70 ± 1.09	195.5 ± 0.26	−38.9 ± 0.32
10	17.425	TPGS	92 ± 0.92	122 ± 0.12	−34.5 ± 0.34
11	55	TPGS	77 ± 0.66	162.1 ± 0.15	−32.6 ± 0.11
12	55	TPGS	72.19 ± 0.55	163.2 ± 0.22	−34.2 ± 0.14
13	10	P123	69 ± 0.78	192.3 ± 0.42	−37.7 ± 0.25
14	32.5	TPGS	82 ± 0.67	157.6 ± 0.31	−35.3 ± 0.17
15	24.924	TPGS	70 ± 0.83	143 ± 0.19	−40.6 ± 0.26
16	10	TPGS	95 ± 0.33	157.8 ± 0.43	−31.2 ± 0.56
17	10	TPGS	98 ± 0.23	155.8 ± 0.34	−32.3 ± 0.14

Data are given as mean ± SD ($n = 3$)

numerical desirability approach, adhering to the constraints detailed in Table I.

Preparation of Gallic Acid-Loaded Lecithin-Polymer Hybrid Micelles

Lecithin-polymer hybrid micelles (LPHM) were prepared using the thin film hydration technique. Lecithin (135 mg) was dissolved in 2mL methylene chloride, and the polymer (65 mg) was dissolved in 1mL methanol. The appropriate amount of drug (as specified in Table I) was added to the polymer solution. These solutions were combined in a round-bottom flask and rotary evaporator (Heidolph, Germany) at 40°C and 120 rpm for one hour to create a thin film. The film was then hydrated with 10 mL double distilled water for one hour at 40°C. A 0.22 µm filter (Millipore, USA) was used to discard any unentrapped drug, and the resulting micellar dispersion was stored at 4°C [24].

Characterization of the Lecithin-Polymer Hybrid Micelles

Determination of Percentage Entrapment Efficiency (EE %) and Drug Loading (DL%) A known volume of the Lecithin-polymer hybrid micelles (LPHM) was dissolved in methanol for complete disruption of the micelles, and the drug was measured spectrophotometrically using UV spectrophotometer (UV-1700, Shimadzu, Japan). The pre-made calibration curve in methanol was used to calculate the concentration of gallic acid. Every experiment was carried out three times [27].

The EE % was calculated using Eq. (1):

$$EE\% = \frac{\text{amount of gallic acid entrapped}}{\text{total amount of gallic acid}} \times 100 \quad (1)$$

The DL% was calculated using Eq. (2):

$$\text{DL\%} = \frac{\text{Weight of gallic acid in lecithin – polymer hybrid micelles}}{\text{total weight of components in the micellar preparation}} \times 100 \quad (2)$$

Determination of Particle Size and Zeta Potential The average particle size and zeta potential of the produced lecithin-polymer hybrid micelles were measured by dynamic light scattering using a Zetasizer sizer (Malvern Instruments, Malvern, UK). The measurements were performed at 25°C with a constant angle of 90°. Each measurement was carried out in triplicate [28, 29].

Optimization of Lecithin-Polymer Hybrid Micelles

Based on constraints outlined in Table I , Design Expert software proposed an optimized formula for lecithin-polymer hybrid micelles. The optimization criteria included maximizing EE%, minimizing PS, and maximizing zeta potential. The validity of the experimental design was then verified by preparing and characterizing the optimized formula (O1).

Transmission Electron Microscopy (TEM)

Transmission electron microscopy (TEM) was used to inspect the surface morphology of the prepared lecithin-polymer hybrid micelles. The procedure involved placing a sample drop onto a coated carbon copper grid to create a thin film. This film was subsequently stained with phosphotungstic acid and allowed to dry completely before morphological analysis using TEM. (JEM-1400 JEOL, Tokyo, Japan) [30, 31].

In-Vitro drug Release

The dialysis bag method was used to evaluate the *in vitro* drug release of the optimized formula as compared to the standard gallic acid. Before being used, a dialysis membrane (Spectrum Medical Inc., Los Angeles, CA, USA) with a molecular weight cut-off between 12,000 and 14,000 Da was thoroughly cleaned with boiling water and soaked in the release medium for the entire night. The dialysis bags were then loaded with a predetermined volume of the optimized formula or a gallic acid suspension (equivalent to 1.5 mg of gallic acid) and subsequently immersed in containers containing 100 mL of phosphate-buffered saline (pH 6.8) [32]. The containers were maintained in a thermostatically regulated shaking water bath at 37°C and 100 rpm. At specific time intervals (0.1667, 0.33, 0.5, 1, 2, 3, 4, 5, 6, and 24 h), two mL samples were obtained and quickly replaced with an equivalent volume of new dissolving medium to maintain sink conditions. After passing through a Millipore membrane filter, the samples were examined at the specified wavelength using a spectrophotometer (Shimadzu Corporation, UV-1800, 240 V, Japan) [33]. The percentage of cumulative gallic acid release at each time interval was calculated using the following Eq. (3):

$$\%\ Cumulative\ release = \frac{(Amount\ of\ GA\ in\ medium)}{(Amount\ of\ GA\ in\ the\ micelles)} \times 100 \quad (3)$$

Drug release kinetics were assessed by applying five mathematical models, namely zero-order, first-order, Korsmeyer–Peppas, Weibull, and Hixson–Crowell, using KinetDS 3.0® as the analytical tool [34].

Stability Studies

Storage Conditions The stability of the optimized formula was evaluated under two storage conditions. Samples were stored for three months at 4°C with a relative humidity of 55–60%, and for one month at room temperature (25 ± 2°C) [35]. Following this storage period, visual inspection and measurements of key parameters: particle size, PDI, zeta potential, drug loading and entrapment efficiency % were carried out [36]. All measurements were performed in triplicate, and the results are reported as mean ± SD.

Stability in Simulated Gastric and Intestinal Fluids The stability of the developed optimized micelles in media simulating physiological conditions of the gastrointestinal tract was evaluated. The optimized formula was diluted tenfold with simulated gastric fluid (SGF, pH 1.6) and simulated intestinal fluid (SIF, pH 6.5), and incubated at 37°C. At predetermined time intervals (2, 4, 6, 8, and 12 h), samples were analysed for particle size. All experiments were performed in triplicate, and the mean ± SD values are reported ($n = 3$) [37].

Pharmacokinetics Study

Chromatographic System and mass Spectrometric Conditions

A Thermo Fisher Scientific Accela 1250 UHPLC system and a TSQ Quantum ultra triple quadrupole mass spectrometer (LC–MS/MS system) were used for the analysis. A Cyano Phenomenex column (4.6 × 50 mm, 5 µm particle size) was used to accomplish chromatographic separation. The mobile phase was made up of 0.25% formic acid in a 90:10 v/v mixture of water to methanol. The injection volume was 5 µL, the column temperature was set at 25°C, and the flow rate was 200 µL/min. Analyst 1.7.2 software (AB SCIEX, Canada) was used to acquire the data. GA and IS were quantified using mass spectrometry in multiple reaction monitoring (MRM) mode using negative electrospray ionization (ESI). For GA and IS, the observed ion transitions were m/z 169.181 → 125.268 and m/z 326.922 → 192.167, respectively. The collision gas

used in collision-induced dissociation (CID) was helium [38]. Sheath gas flow rate: 40 AU; auxiliary gas flow rate: 10 AU; spray voltage: 2500 V; vaporizer temperature: 350°C and capillary temperature: 350°C.

Solutions Preparation

A stock solution containing 20 µg/mL of gallic acid (GA) was dissolved in methanol. Methanol was used as a solvent to dilute the stock solution to create the working solutions (0.5–16 ng/mL). Prior to analysis, all of the prepared solutions were kept at 4°C.

Plasma Sample Preparation

Plasma gallic acid quantification was carried out based on a previously published and validated UHPLC–MS/MS method [38] with modifications tailored to our experimental conditions. In our study, the sample preparation workflow was adapted as follows: 200 µL of plasma was spiked with 50 µL of gallic acid and internal standard solution (20 µg/mL) in an Eppendorf tube and vortexed for 60 s. Protein precipitation was achieved using 200 µL of trifluoroacetic acid, after which the mixture was centrifuged at 12,000 rpm for 10 min. The resulting supernatant was carefully collected, filtered, and directly injected into the LC–MS/MS system for analysis. These modifications were made to optimize sample preparation and chromatographic performance for our study while maintaining the overall structure of the validated method.

In-Vivo Pharmacokinetics Study

Twelve rats were split into two groups ($n=6$) for the *in-vivo* pharmacokinetics investigation. The first group (GA) received standard gallic acid, and the second group (O1) received the optimized formula. Animals were allowed free access to water throughout a 12-h fast. The GA group received a dose of 20 mg/kg of gallic acid, prepared as a suspension in water (standard GA). The O1 group received a corresponding dose (20 mg/kg) of the O1 formula. The drug was administered orally through an intragastric tube. Blood samples were taken from the retro-orbital plexus at 10, 30, 60, 90, 120, 180, 240, 300, and 1440 min after administration, collected in heparinized tubes, and immediately centrifuged at 13,000 × g for 10 min at 4°C. After that, the plasma was kept at −80°C until HPLC analysis. Using non-compartmental analysis and Kinetica TM 2000 software (version 4.4.1, Thermo Electron Corporation, USA), pharmacokinetic parameters were obtained (Rideau *et al*., 2018).

In-Vivo Pharmacodynamics Study

Induction of Pulmonary Fibrosis

To induce pulmonary fibrosis in rats, an intratracheal administration of bleomycin sulfate at a dose of 5 mg/kg was performed once under anaesthesia using xylazine (20 mg/kg, intraperitoneally) and ketamine (80 mg/kg, intraperitoneally). The bleomycin dosage was selected according to a prior study [39, 40].

Experimental Design

Rats were divided randomly into five groups ($n=6$). The first group was the sham-operated control, while the second group (bleomycin control) received an intratracheal injection of bleomycin (5 mg/kg). The third group was administered the blank formulation for 21 days starting on the day of induction. The fourth group received a gallic acid suspension (20 mg/kg, orally), and the fifth group was administered optimized gallic acid formulation at the same dose for 21 consecutive days following bleomycin administration. Finally, all animals were anesthetized and euthanized via cervical dislocation. Lungs were promptly excised for subsequent biochemical analyses and histopathological evaluation.

Biochemical Assays

In the lung tissue, hydroxyproline concentration was measured using a standard colorimetric assay kit (Cat. No. K555-100; Biovision Inc., CA, USA). Pulmonary levels of transforming growth factor-β (TGF-β), matrix metalloproteinase-7 (MMP-7), and collagen type I were measured by ELISA following the manufacturers' protocols, employing the respective kits (Cat. No. SEA124Ra; Cloud-Clone Corp., TX, USA, and Cat. Nos. NBP3-06896 and NBP2-7582; Novus Biologicals, LLC, USA).

Histopathological Examination of lung Tissue

Lung specimens from all experimental groups were thoroughly rinsed and subsequently fixed in 10% neutral buffered formalin for 72 h. Afterwards, tissues were trimmed and subjected to dehydration through ascending concentrations of ethanol, cleared in xylene, and re-infiltrated with graded alcohols. Thereafter, samples were embedded in Paraplast tissue embedding medium. A rotary microtome was used to produce 5 µm thick slices, which were then stained with Masson's trichrome (Leica Microsystems GmbH, Wetzlar, Germany) prior to histological evaluation under a light microscope. The extent of collagen deposition in lung tissue was quantified using ImageJ software (Version fiji-stable-win64-jdk, USA) by applying colour deconvolution to

isolate the stain, followed by thresholding and measurement of the percentage area occupied by collagen.

Statistical Analysis

Optimization data were determined statistically using Design-Expert 13.0.5.0® software (Stat-Ease Inc., Minneapolis, USA) employing linear regression and ANOVA. The evaluation involved comparing the coefficient of variation (CV), R^2, adjusted R^2, and predicted R^2 values. Statistical significance was confirmed with a p-value less than 0.05.

Data on stability, *in vivo* pharmacokinetics, and pharmacodynamics are expressed as mean ± SEM. One-way ANOVA was used to evaluate differences between experimental groups, and the Tukey–Kramer post hoc test was used for multiple comparisons. The statistical significance was considered at $p < 0.05$. GraphPad Prism version 6 was used for all statistical analyses (GraphPad Software, Inc., USA).

Results and Discussion

Authentication and Structure Elucidation of Gallic Acid

After several chromatographic isolation procedures, an off-white amorphous powder (915 mg) was obtained, having a melting point of 258°C and was soluble in methanol. This compound had a retardation factor (R_f) value of 0.73 on TLC plates when eluted with a solvent composed of [dichloromethane—methanol (90:10 v/v)]. The compound appeared as an intense violet spot on paper chromatography under short UV light (254nm) having R_f values of 52 and 81 when developed using distilled water and n-butanol – acetic acid – water (4:1:5) (upper phase) solvent system respectively. The spots gave intense bluish violet colour when sprayed with ferric chloride. For further identification of the compound, its UV absorption spectrum exhibited one intense peak at λ_{max} (methanol) 272 nm. ^{1}HNMR spectrum of the isolated compound, as shown in supplementary fig. (S1), portrays distinctive sharp and intense peak [^{1}HNMR (600 MHz, CD3OD): δ 7.11 (s, 2H, ArH), representing protons (H-2 and H-6). Moreover, the FTIR spectrum revealed the presence of different functional groups that were recognized through various bending and stretching vibrations as shown in supplementary fig. (S2). The spectrum revealed the presence of carboxylic group (3408.22 and 3496.94 cm^{-1}), band at (1676.14 cm^{-1}) corresponding to a C = O bond tension and a very broad band (2503.6 cm^{-1}) of the O–H stretching that specified the existence of the carboxylic group. Aromatic ring vibration (C = C) stretching can be observed at (1541.12 cm^{-1}). There was a C-O stretching of carboxylic acid band observed at (1255.66 cm^{-1}) Two O–H deformation bending bands can be observed at (1384.89 cm^{-1}) and (864.11 cm^{-1}). These data were consistent with those of gallic acid, so its identification was confirmed by co-chromatography with authentic gallic acid on paper chromatography using n-butanol – acetic acid – water (4:1:5) (upper phase) solvent system. Thus, the compound could be identified as 3,4,5-trihydroxybenzoic acid (Gallic acid) ($C_7H_6O_5$).

Preparation of Gallic Acid-Loaded Lecithin-Polymer Hybrid Micelles

According to previous studies, Pluronic® P123 and TPGS were identified as suitable amphiphilic polymers for combination with lecithin. Their favourable physicochemical properties, particularly their hydrophilic–lipophilic balance (HLB) values of 8 and 13.2, respectively, render them highly compatible with lecithin. Higher gallic acid loading without precipitation is achieved by this compatibility encouraging the self-assembly of stable mixed micelles with sufficient core volume [41, 42]. Pluronic®P123 exhibits a unique self-assembling property, forming spherical micelles characterized by a hydrophilic PEO outer shell, conferring dispersion stability, and a hydrophobic PPO inner core, providing a reservoir for hydrophobic agents [43]. The triblock architecture of Pluronic.® P123 facilitates effective integration within the hydrophobic core, maximizing the encapsulation of hydrophobic drugs and simultaneously providing steric stabilization against micelle aggregation [25].

TPGS is water-soluble and a natural derivative of vitamin E. It combines the benefits of both PEG and vitamin E for drug delivery applications using nanocarriers. These benefits include extended drug half-life in plasma and improved cellular uptake [44]. Its structure comprises a hydrophilic polar head and a lipophilic alkyl tail (amphiphilic) (HLB 13.2, CMC 0.02% w/w), making TPGS an optimum micelle-like biomaterial for various drug delivery systems. TPGS enables prolonged, controlled, and targeted drug delivery, helps to overcome multidrug resistance (MDR), and improves drug absorption orally by inhibiting P-glycoprotein (P-gp) [45].

Statistical Analysis Using D-optimal Design

A D-optimal experimental design was used to assess the effects of formulation factors. Because of its shown effectiveness in lowering the variance of predicted model coefficients, this design was selected [46, 47]. The resulting design comprised 17 experimental runs, with the results for encapsulation efficiency (% EE), particle size, and zeta potential summarized in Table I. The optimized formula was selected to achieve highest % EE and zeta potential, in addition to a minimum particle size.

The experimental design supported the fifth models for the measured responses, as can be shown from Table II and Fig. 1. The fitted models were characterised by a high correlation coefficient R^2, and an adjusted R^2 in close agreement to the predicted R^2, as well as enough precision values of 0.9816, 0.9733, 0.9655, 41.019, respectively for EE %, 0.9969, 0.9955, 0.9939, 85.784 for the particle size, and 0.8790, 0.8240, 0.7488, 13.9143 respectively for the zeta potential. The following are the regression equations that were obtained for the responses:

$$\begin{aligned} \mathrm{EE\%}\ (Y_1) = {} & 70.5 + 47.7054 * X_1 - 12.5 * X_2 + 9.29647 \\ & * X_1X_2 - 5.69195 * X_{1^2} + 104.774 * X_{1^2}X_2 \\ & - 336.169 * X_{1^3} - 3.02824 * X_{1^3}X_2 + 15.0831 \\ & * X_{1^4} - 99.4095 * X_{1^4}X_2 + 284759 * X_{1^5} \end{aligned} \quad (4)$$

$$\begin{aligned} \mathrm{PS}\ (Y_2) = {} & 150.925 - 8.92944 * X_1 - 4.375 * X_2 \\ & - 5.43541 * X_1X_2 + 50.1896 * X_{1^2} + 182.601 \\ & * X_{1^2}X_2 + 20.659 * X_{1^3} - 0.01667 * X_{1^3}X_2 \\ & - 28.675 * X_{1^4} - 166.086 * X_{1^4}X_2 - 13.5316 * X_{1^5} \end{aligned} \quad (5)$$

$$\begin{aligned} \mathrm{ZP}\ (Y_3) = {} & 36.6 - 16.1329 * X_1 + 0.95 * X_2 + 2.97453 \\ & * X_1X_2 - 2.49678 * X_{1^2} - 4.64906 * X_{1^2}X_2 \\ & + 66.258 * X_{1^3} - 4.04536 * X_{1^3}X_2 + 0.492611 \\ & * X_{1^4} + 5.29072 * X_{1^4}X_2 - 50.3168 * X_{1^5} \end{aligned} \quad (6)$$

A positive coefficient indicated that the factor enhanced the studied response (synergistic effect), whereas a negative coefficient indicated an inhibitory effect (antagonistic effect). The absolute value of the coefficient reflected the strength of the factor's influence; larger coefficients corresponded to a greater impact on the response [29, 48, 49].

Entrapment Efficiency % Analysis

The EE% for all formulae ranged from was between $48 \pm 0.45\%$ to $98 \pm 0.23\%$ (Table I). The drug loading for all formulae ranged within 3.45 ± 0.37 to $21.17 \pm 0.42\%$ (results not shown). As shown in Table II, the drug amount (X_1) had a significant effect on the EE% as shown by its p-value. By referring to Eq. 4, it was found that the drug amount (X_1) had a synergistic effect on increasing the EE% due to its positive coefficient. The observed increase in EE% with increasing drug amount can be attributed to enhanced drug availability for encapsulation. This increased availability may contribute to both better EE% and greater of drug retention within the micellar structure [28].

As shown in Table II, the type of polymer had a significant impact on the EE% as shown by its p-value. By referring to Eq. 4 it was found that TPGS had a significant effect on increasing the EE% as shown by its negative coefficient (X_2). The superior entrapment efficiency (EE%) achieved with TPGS-based micelles can be attributed to the favourable match between the moderate hydrophilicity of gallic acid ($\log P \approx 0.7–1$) [50] and the amphiphilic nature of TPGS (HLB = 13.2) which facilitates efficient drug incorporation into the micellar core while maintaining colloidal stability [22]. By contrast, Pluronic P123, with a lower HLB value of 8, exhibits greater hydrophobicity, favouring the encapsulation of highly lipophilic agents but showing reduced compatibility with moderately hydrophilic compounds such as gallic acid [51]. The enhanced EE% observed with TPGS can also be explained by its intrinsic solubilizing capacity. TPGS, composed of polyethylene glycol (PEG) esterified with vitamin E, has a low CMC ($\approx 0.02\%$ w/w), which contributes to its effectiveness in enhancing the solubility of poorly soluble drugs and its loading efficiency [52, 53]. Another reason for the increase in EE % with TPGS is that it has been reported that TPGS forms strong hydrophobic interactions with hydrophobic drugs within the micellar core [27, 54].

Particle Size Analysis

The particle size for all formulae ranged from 122 ± 0.12 nm to 198.2 ± 0.16 nm as shown in Table I. Also, it was clear from Table 2 that the type of polymer had a significant impact on the particle size as shown by its p-value. By referring to Eq. 5, it was found that TPGS had a significant effect on increasing the particle size due to its negative coefficient (X_2). The significant observed particle size enlargement with TPGS ($p < 0.0001$) is likely because of the incorporation of its hydrophobic components into the micellar structure, which resulted in increased micellar core size which in turn resulted in increased entrapment efficiency % as discussed earlier [55–57]. This finding is consistent with previous research [29].

Zeta Potential Analysis

Colloidal dispersions stability is crucially assessed by measuring Zeta potential [58]. The zeta potential for all formulae ranged from $-31.2 \pm 0.56\%$ to—$40.6 \pm 0.26\%$ as shown in Table I. The observed high zeta potential, indicating strong electrostatic repulsion between similarly charged particles, suggests good stability of the prepared lecithin-polymer hybrid micelles. The negative charge seen in all the formulas is due to lecithin, an ampholytic surfactant that has phosphate groups carrying negative charges [59, 60]. This anionic nature of lecithin is thus responsible for the high negative zeta potential observed across all formulations, as both TPGS and Pluronic® P123 are non-ionic [61].

TableII ANOVA Table for the Measured Responses

Source	EE %					Particle size					Zeta potential				
	Sum of Squares	df	Mean Square	F-value	p-value	Sum of Squares	df	Mean Square	F-value	p-value	Sum of Squares	df	Mean Square	F-value	p-value
Block	65.66	1	65.66			17.8	1	17.8			0.2306	1	0.2306		
Model	4892.28	10	489.23	117.67	< 0.0001	16,288.3	10	1628.83	703.5	< 0.0001	143.73	10	14.37	15.98	< 0.0001
X1-Drug amount	218.18	1	218.18	52.48	< 0.0001	7.64	1	7.64	3.3	0.0829	24.95	1	24.95	27.74	< 0.0001
X2-Type of polymer	625	1	625	150.32	< 0.0001	76.56	1	76.56	33.07	< 0.0001	3.61	1	3.61	4.01	0.0576
X1X2	103	1	103	24.77	< 0.0001	35.21	1	35.21	15.21	0.0008	10.55	1	10.55	11.72	0.0024
$X1^2$	3.14	1	3.14	0.7563	0.3939	244.48	1	244.48	105.59	< 0.0001	0.605	1	0.605	0.6727	0.4209
$X1^2X2$	1065.42	1	1065.42	256.25	< 0.0001	3236.11	1	3236.11	1397.7	< 0.0001	2.1	1	2.1	2.33	0.141
$X1^3$	505.74	1	505.74	121.64	< 0.0001	1.91	1	1.91	0.8249	0.3736	19.65	1	19.65	21.84	0.0001
$X1^3X2$	9.88	1	9.88	2.38	0.1375	0.0003	1	0.0003	0.0001	0.991	17.63	1	17.63	19.6	0.0002
$X1^4$	28.36	1	28.36	6.82	0.0159	102.49	1	102.49	44.27	< 0.0001	0.0302	1	0.0302	0.0336	0.8562
$X1^4X2$	1231.77	1	1231.77	296.26	< 0.0001	3438.28	1	3438.28	1485.01	< 0.0001	3.49	1	3.49	3.88	0.0616
$X1^5$	579.69	1	579.69	139.43	< 0.0001	1.31	1	1.31	0.5654	0.4601	18.1	1	18.1	20.12	0.0002
Residual	91.47	22	4.16			50.94	22	2.32			19.79	22	0.8994		
Lack of Fit	43.11	10	4.31	1.07	0.4492	29.19	10	2.92	1.61	0.2149	12.5	10	1.25	2.06	0.1183
Pure Error	48.35	12	4.03			21.75	12	1.81			7.29	12	0.6075		
Cor Total	5049.41	33				16,357.04	33				163.74	33			

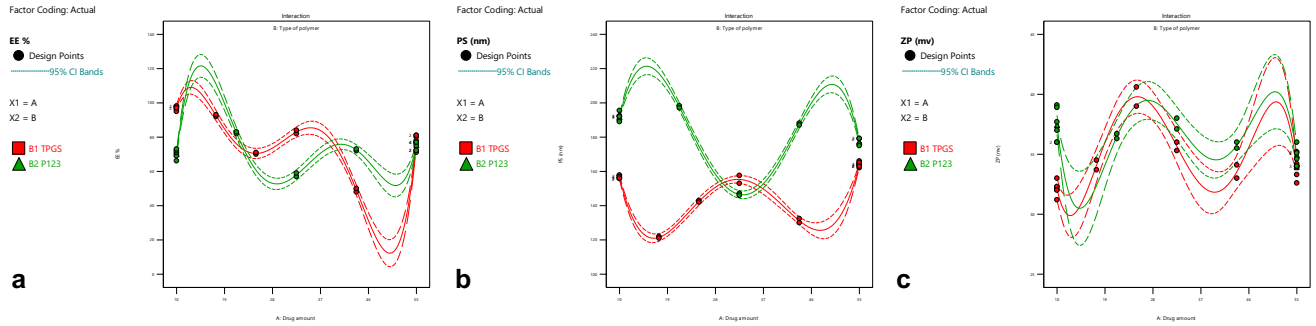

Fig. 1 Interaction plot showing the fifth effect of drug amount and type of polymer on **a**: Entrapment efficiency %, **b**: Particle size and **c**: Zeta potential

Analysis of the data in Table II and Eq. 6 indicates a statistically significant correlation between the drug amount (X_1) and the zeta potential, demonstrating that increasing X_1 resulted in a concomitant decrease in the negative charge which means higher zeta potential (Eq. (6)). The increase in the zeta potential with increasing drug amount could be attributed to the fact that gallic acid molecule has a carboxylic acid group, and three hydroxyl groups, and when prepared in slightly neutral medium, they show a negative zeta potential due to deprotonation from both the carboxylate and hydroxyl groups [62].

Formulation Optimization

Design Expert® software was employed to optimize gallic acid-loaded lecithin-polymer hybrid micelles by identifying the formulation exhibiting the maximum encapsulation efficiency (EE%), highest zeta potential, and the minimal particle size. Table III details the optimized formula composition alongside the anticipated and experimentally observed values for these responses. The optimized formula showed a drug loading % of 8.23 ± 1.07%, an entrapment efficiency of 96.78 ± 1.45%, a particle size of 120.22 ± 1.45 nm, and a zeta potential of − 32.12 ± 0.97 mV. The minimal prediction error observed across all responses (as presented in Table III) confirms robustness and reliability of the applied experimental design for the preparation and optimization of gallic acid-loaded lecithin-polymer hybrid micelles.

Transmission Electron Microscopy Analysis

Transmission electron microscopy was used to determine the structure of the optimized formula. Transmission electron microscopy revealed a spherical morphology with no signs of aggregation as shown in Fig. 2a [25]. However, particle size analysis revealed a difference between TEM and zeta sizer measurements. This difference is inherent to the techniques employed: TEM analyses dehydrated samples, providing a direct measurement of particle diameter, while dynamic light scattering determines the hydrodynamic diameter, which includes the solvation shell. This hydration layer accounts for the larger particle sizes obtained via dynamic light scattering [63].

In-Vitro drug Release

A distinct difference in the release profile of gallic acid was observed between the optimized formulation and free GA (Fig. 2b). The optimized formula exhibited a significantly slower release, with only 41.23 ± 2.03% released after 0.5 h, compared with 92.58 ± 1.45% for the standard GA. The release from the optimized formula gradually increased over time, reaching 80 ± 1.09% after 24 h. The release pattern exhibited two phases: an initial rapid and a prolonged steady release afterwards [49]. The produced micelles' nanoscale size, which offers a huge surface area for solvent interaction, is probably what caused the first rapid drug release

Table III The Composition of the Optimised Formula As Suggested By Design Expert Software, the Predicted and Observed Results

Optimized formula Composition	Response	Predicted	Observed	Prediction error %*	Desirability
Drug amount (mg): 17	EE%	95.35	96.78 ± 1.45	1.49	0.855
Type of polymer: TPGS	PS	121.08	120.22 ± 1.45	0.71	
	ZP	−33.40	−32.12 ± 0.97	3.83	

*Prediction error % = ((Predicted- Observed)/Predicted)*100

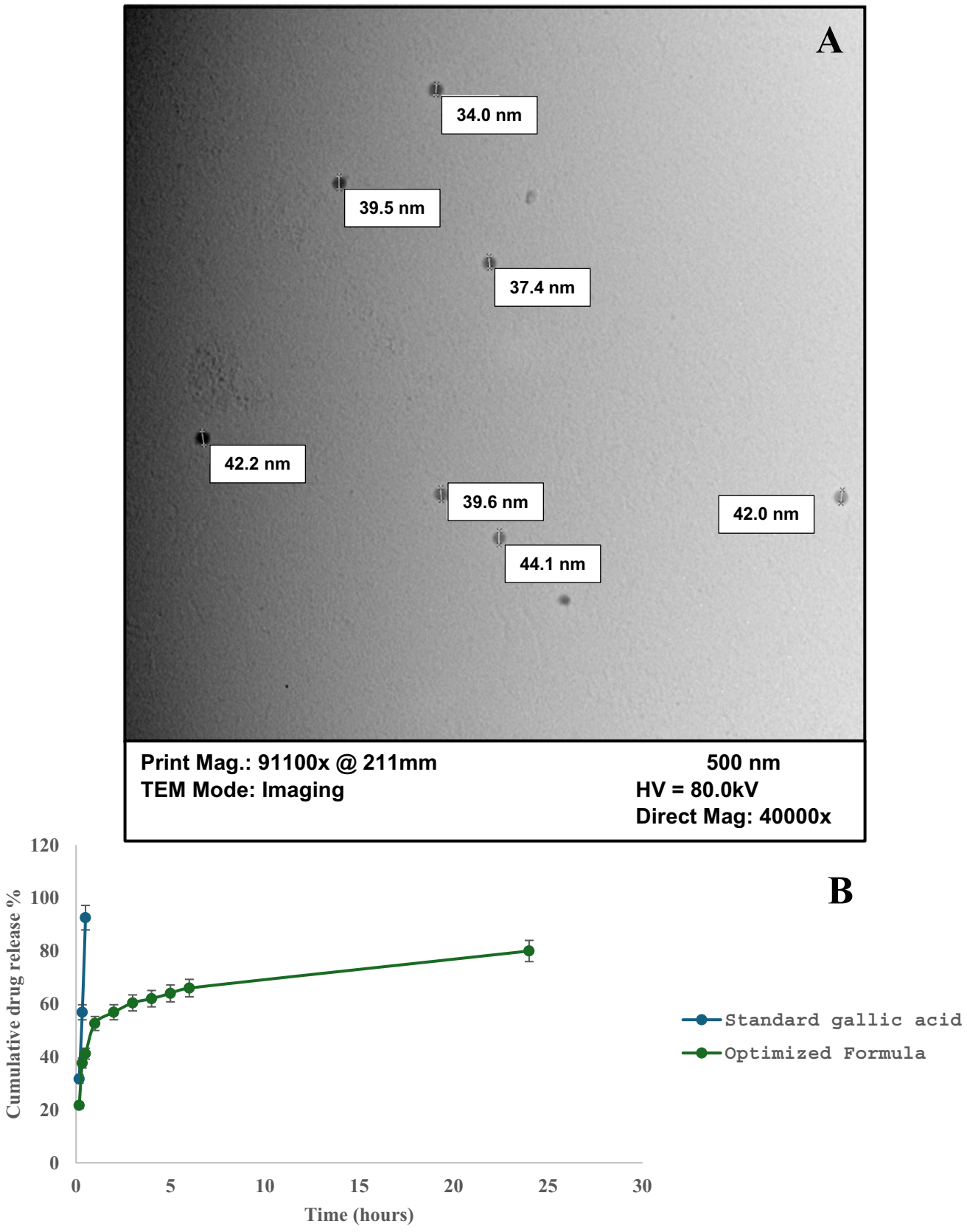

Fig. 2 **A** TEM images of optimized formula **B** Release rate of optimized formula as compared to the standard gallic acid in simulated intestinal fluid (pH 6.8) ($n=3$)

[27], as well as the presence of drug molecules positioned at the interface of the hydrophobic core and hydrophilic corona, which are more readily liberated upon hydration and passive diffusion. The subsequent sustained release can be attributed to strong hydrophobic interactions within the phospholipid bilayer, stabilized by TPGS, which enhance drug–carrier association and retard gallic acid diffusion [29, 64, 65]. Such sustained release profiles can be advantageous in treating pulmonary fibrosis by maintaining a consistent gallic acid concentration within pulmonary tissues.

Upon fitting the release data to various kinetic models, the zero-order, first-order, Korsmeyer–Peppas, Weibull, and Hixson–Crowell it yielded correlation coefficients (R^2) of 0.4059, 0.0514, 0.9750, 0.9802, and 0.1638, respectively. Among these, the Weibull model demonstrated the strongest correlation, indicating that it most appropriately describes the release behaviour of gallic acid from lecithin-based micelles. The value of ß in the Wiebull model indicated the release mechanism. In our study, ß was greater than 1, indicating a sigmoidal release profile [66]. This release profile can be explained by the structural and dynamic properties of TPGS–lecithin mixed micelles. In such systems, drug release is governed by multiple, time-dependent processes rather than a single diffusion mechanism, which naturally gives rise to a non-monotonic release rate [24]. Initially, the encapsulated drug is retained within a highly organized hydrophobic core formed by the tocopherol moiety of TPGS and the lipid chains of lecithin. This compact core limits immediate diffusion, resulting in a slow initial release phase. As the micelles interact with the release medium, gradual water penetration, micellar swelling, and partial lipid rearrangement occur. These structural changes increase core permeability and facilitate drug diffusion, leading to an accelerated release phase [67]. As release progresses further, the system approaches a new equilibrium characterized by drug depletion, reduced concentration gradients, and increased micellar stability under dilution, causing the release rate to decline asymptotically. This sequence—initial retardation, acceleration due to micellar reorganization, and eventual deceleration—is captured mathematically by the sigmoidal Weibull function with ß > 1. Thus, the Weibull shape parameter reflects the combined effects of diffusion, micelle restructuring, and partial disassembly inherent to TPGS–lecithin mixed micelles, rather than simple Fickian diffusion alone.

Stability Studies

Storage Conditions

The stability of the optimized micellar formulation was evaluated under two storage conditions. At both storage conditions, stability was confirmed by the absence of sedimentation or particle aggregation during monthly visual assessments. No significant changes were observed in mean particle diameter, PDI, zeta potential, or encapsulation efficiency % over three months at 4°C, with final values of 120.65 ± 0.17 nm, 0.23 ± 0.11, –31.47 ± 0.37 mV, and 95.12 ± 0.21%, respectively. At room temperature (25 ± 2°C), the formulation was stable for one month, with mean diameter, PDI, zeta potential, drug loading and encapsulation efficiency % values of 122.18 ± 0.21 nm, 0.25 ± 0.09, –30.82 ± 0.42 mV, 8.05 ± 0.13 and 94.78 ± 0.18%, respectively. These results indicate that the micellar system maintains its physical and chemical integrity under both refrigerated and ambient conditions.

Stability in Simulated Gastric and Intestinal Fluids

To ensure effective delivery of the encapsulated drug to its absorption site, the micelles must resist rapid dissociation upon dilution and exposure to the harsh conditions of the gastrointestinal tract. Therefore, the stability of the optimized formula was evaluated at 37°C in simulated gastric fluid (SGF, pH 1.6) and simulated intestinal fluid (SIF, pH 6.5) over 12 h. As shown in Table 1S, the particle size of the micelle size remained unchanged in both SGF and SIF over the respective incubation periods, with no significant variation observed. These results indicate that optimized formula is expected to remain stable in gastrointestinal fluids throughout the absorption period. This results were in accordance with Jadhav *et al.,* 2016 [37].

Pharmacokinetics Analysis

Method Development and Optimization

The chromatographic conditions were optimized by adjusting the mobile phase to improve peak separation and reduce analysis run time, without compromising electrospray ionization efficiency. Methanol was chosen as the organic modifier to obtain better peak symmetry and high sensitivity, while 0.25% formic acid was added to improve separation and enhance the ionization. The optimized separation employed an isocratic elution with 0.25% formic acid in water: methanol (90:10 v/v %), producing well-resolved sharp peaks with retention time of 3.06 ± 0.02 For IS and 1.96 ± 0.05 for GA. Figure 3A and B show the MRM chromatograms of dapagliflozin (Internal standard) and gallic acid, respectively.

A good linearity was obtained in the range of (0.5—16 ng/mL) in spiked human plasma. Linear regression analysis yielded Eq. 7:

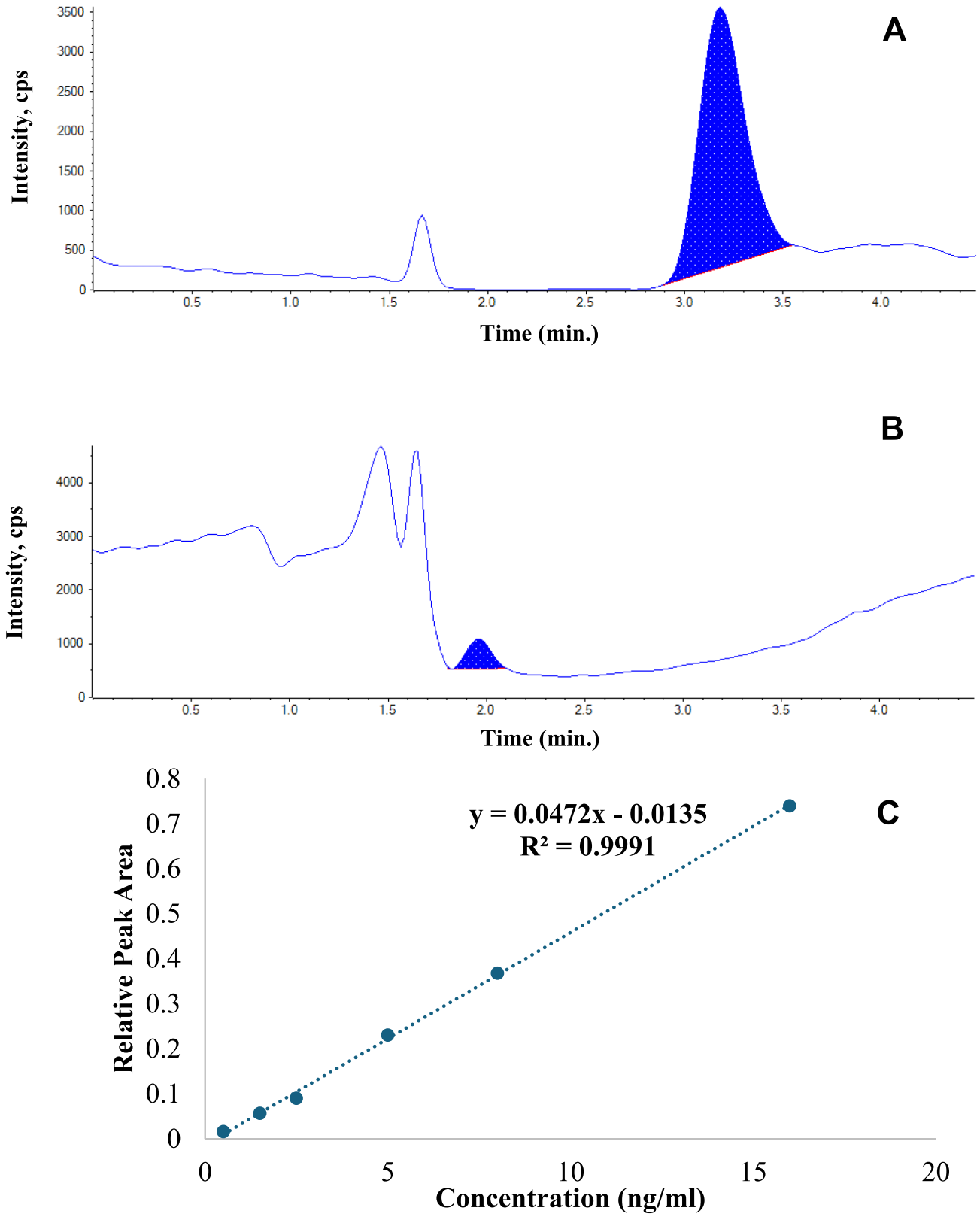

Fig. 3 MRM Chromatogram of **A** dapagliflozin (Internal standard) and **B** MRM Chromatogram of Gallic acid (2.5 µg/ml) in spiked human plasma **C** Calibration curve of gallic acid with concentration range (0.5–16 ng/ml) against relative peak area

Table IV Pharmacokinetic Parameters of Standard Gallic Acid and Optimized Formula

Parameter	Standard Gallic acid	Optimized formula
C_{max} (ng/mL)	1315.75 ± 13.54	2150.460 ± 21.74[a]
T_{max} (min)	30 ± 0.15	30 ± 0.27
AUC $_{0-24}$ (ng/min/mL)	151,073.868 ± 56.22	1,111,506.392 ± 971.76[a]
AUC $_{0-\infty}$ (ng/min/mL)	163,541.934 ± 107.13	2,099,820.316 ± 855.22[a]
AUMC $_{0-24}$(ng/min^2/mL)	50,817,157.628 ± 201.11	651,644,778.104 ± 945.43[a]
AUMC $_{0-\infty}$ (ng/min^2/mL)	76,618,838.606 ± 1054.22	4,038,033,986.169 ± 1234.76[a]
Mean Residence time (min)	468.4965 ± 23.78	1923.037 ± 25.76 [a]

Cmax peak plasma concentration, *Tmax* time to reach peak plasma concentration, *AUC 0–24* area under the plasma concentration–time curve from time 0 to 24 h, *AUC 0–∞* area under the plasma concentration–time curve calculated by the linear trapezoidal rule from time 0 to infinity, *AUMC0–24* area under the first moment curve from time 0 to 24 h, *AUMC0–∞* area under the first moment curve from time 0 to infinity

[a] Significant difference from standard gallic acid group. Data is presented as mean ± SEM

$$Y = 0.04723X - 0.0135 \quad (7)$$

where Y is peak area ratio and X is the concentration in plasma. The correlation coefficient is 0.9991 (Fig. 3C) validating the method's quantitative reliability.

In-Vivo Pharmacokinetics Analysis

In rats, the improved formula's oral bioavailability of gallic acid was assessed in contrast with the drug's pure form. Key pharmacokinetic parameters are presented in Table 4, and the average plasma concentration over time for both the optimized formula and standard gallic acid are shown in Fig. 4. The optimized formula showed a significantly higher C_{max} (1.63-fold increase) compared to standard gallic acid, indicating enhanced absorption. The t_{max} was 30 min for both standard and optimized formula.

Formulating gallic acid within a micellar nano-carrier is proposed to improve its solubility and absorption through several pathways. The hydrophobic core of the micelle is thought to aid in the solubilization of gallic acid. Furthermore, due to their amphiphilic nature, the incorporated polymers exhibit surfactant-like behaviour, providing the micelles with enhanced stability and biocompatibility [24].

The AUC_{0-24} for the optimized formula was significantly higher than the observed standard drug (1,111,506.392 ng h/mL *vs*. 151,073.868 ng h/mL, respectively). This resulted in a relative bioavailability of approximately 735% for the optimized formula, indicating that administering the drug in the form of lecithin-polymer hybrid micelles led to a substantial increase in the amount of drug reaching systemic circulation. The enhanced bioavailability typically observed with optimized lecithin-polymer hybrid micelles can be attributed to lecithin presence, a complex phospholipids mixture and fundamental cellular membranes constituents which facilitates gallic acid absorption. Additionally, the amphiphilic phospholipids act as a vesicular carrier, potentially shielding gallic from significant hepatic first-pass metabolism [68].

The mean residence time for the optimized formula was 4.1 folds higher than that for the standard gallic acid. This is possibly due to sustained-release characteristics of micellar formulation which extend gallic acid's systemic circulation time and exposure. Furthermore, the small size of the particles enables them to remain in bloodstream longer because

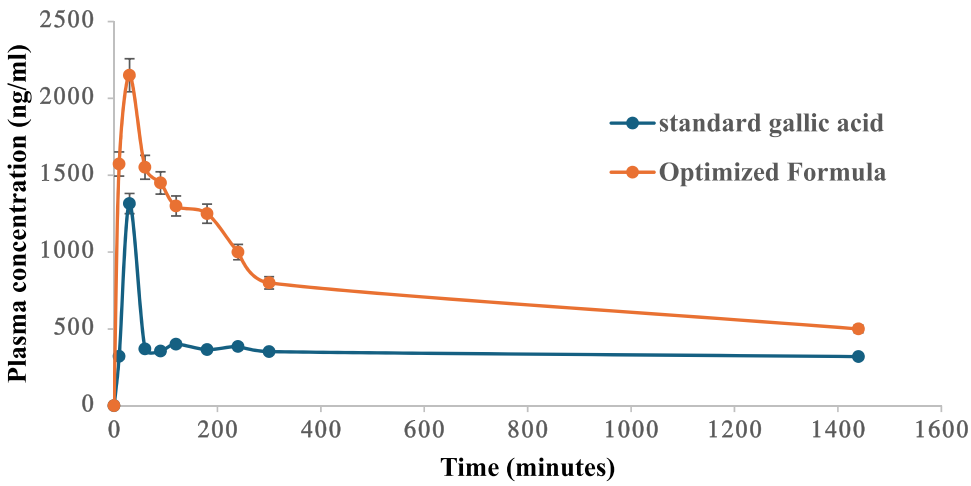

Fig. 4 Mean plasma concentration–time curve of gallic acid after oral administration

they are not easily detected and removed by the reticuloendothelial system (RES). The enhanced time through which the drug circulates enables reaching its target site more effectively, ultimately improving its bioavailability [25, 69]. Moreover, the core–shell structure of lecithin-polymer hybrid micelles, with its hydrophilic corona, is likely to reduce serum protein binding, contributing to prolonged retention. Furthermore, TPGS, known as a permeation and absorption enhancer, was reported to inhibit P-glycoprotein (P-gp) mediated efflux and enhancing cellular uptake [65]. These combined attributes—smaller particle size, controlled release, high stability, and enhanced cellular uptake—resulted in prolonged *in-vivo* circulation and hence improved bioavailability for the lecithin-polymer hybrid micelles [64].

In-Vivo Pharmacodynamic Study

Effect on Pulmonary Levels of TGF-β and MMP-7

TGF-β (transforming growth factor-β) signaling pathway is crucial in the development of pulmonary fibrosis. It promotes fibroblast-to-myofibroblast differentiation, stimulates the synthesis of extracellular matrix proteins, suppresses matrix degradation by matrix metalloproteinases, and drives the epithelial-to-mesenchymal transition [70].

Matrix metalloproteinase-7 (MMP-7) has been proposed as a promising peripheral blood biomarker for idiopathic pulmonary fibrosis (IPF). Elevated expression of MMPs, particularly in activated alveolar epithelial cells, is a characteristic feature of IPF lungs. Under normal physiological conditions, MMP-7 is weakly expressed and primarily targets fibrillar collagen for breakdown; nevertheless, during fibrosis, it becomes significantly elevated in reactive alveolar epithelium, suggesting its potential profibrotic role in IPF pathogenesis [71].

According to the current study, the bleomycin control group's pulmonary levels of TGF-β and MMP-7 were significantly higher than those of the sham-operated group. In contrast, the levels of TGF-β and MMP-7 were significantly suppressed in the pulmonary tissue of the gallic acid-treated group when compared to the bleomycin control group and the blank-treated group. Additionally, the enhanced gallic acid formulation significantly reduced the pulmonary TGF-β level as compared to the group treated with the gallic acid suspension and effectively restored the pulmonary level of MMP-7 with a non-significant difference from the sham-operated group (Fig. 5A).

The observed upregulation of pulmonary TGF-β and MMP-7 levels in the bleomycin control group aligns with their established roles in fibrogenic and matrix remodelling pathways during lung injury. The significant attenuation of these profibrotic markers in rats treated with gallic acid underscores its potential modulatory effect on the inflammatory and fibrotic cascade. Previous studies reported the possible antifibrotic potential of gallic acid [10, 72]. Notably, the enhanced gallic acid formulation demonstrated superior efficacy, particularly in normalizing MMP-7 levels to those of the sham-operated group and significantly reducing TGF-β expression compared to the gallic acid suspension group [73]. These results imply that gallic acid, particularly in its enhanced formulation, may have therapeutic implications by protecting against bleomycin-induced lung fibrosis through downregulating important mediators of tissue remodelling and fibrosis.

Effect on Pulmonary Expression Level of Hydroxyproline and Collagen-1

According to the current findings, the bleomycin control group's lung hydroxyproline and collagen-1 contents were significantly higher than those of the sham-operated group. Pulmonary hydroxyproline and collagen-1 were significantly reduced upon treatment with gallic acid. Furthermore, the optimized formula of gallic acid resulted in the restoration of the normal levels of pulmonary hydroxyproline and collagen-1 (Fig. 5B).

The marked elevation in pulmonary hydroxyproline and collagen-1 content observed in the bleomycin control group reflects the characteristic extracellular matrix deposition associated with bleomycin-induced pulmonary fibrosis. Hydroxyproline serves as a biochemical marker for collagen content, as it is a major component of collagen fibres and reflects the extent of fibrotic deposition within tissue. Collagen-1, the predominant form of fibrillar collagen in pulmonary fibrosis, contributes to the structural remodelling of lung parenchyma and is closely associated with impaired pulmonary function in fibrotic diseases. Treatment with gallic acid significantly mitigated these fibrotic markers, indicating its potential anti-fibrotic effect. Notably, administration of the optimized gallic acid formula yielded a more pronounced therapeutic benefit, effectively normalizing hydroxyproline and collagen-1 levels to near baseline values. These findings suggest that gallic acid, particularly in its enhanced formulation, may exert protective effects by attenuating collagen synthesis and deposition key features in pulmonary fibrosis pathophysiology.

Effect on Histopathological Examination of Lung Tissue

Histopathological assessment using Masson trichrome staining revealed differential collagen deposition across experimental groups, providing critical insight into fibrotic progression and therapeutic intervention. Lung tissue from the sham-operated group (Fig. 6A) exhibited intact alveolar architecture with minimal collagen infiltration, indicative of normal pulmonary histology. In contrast, the bleomycin

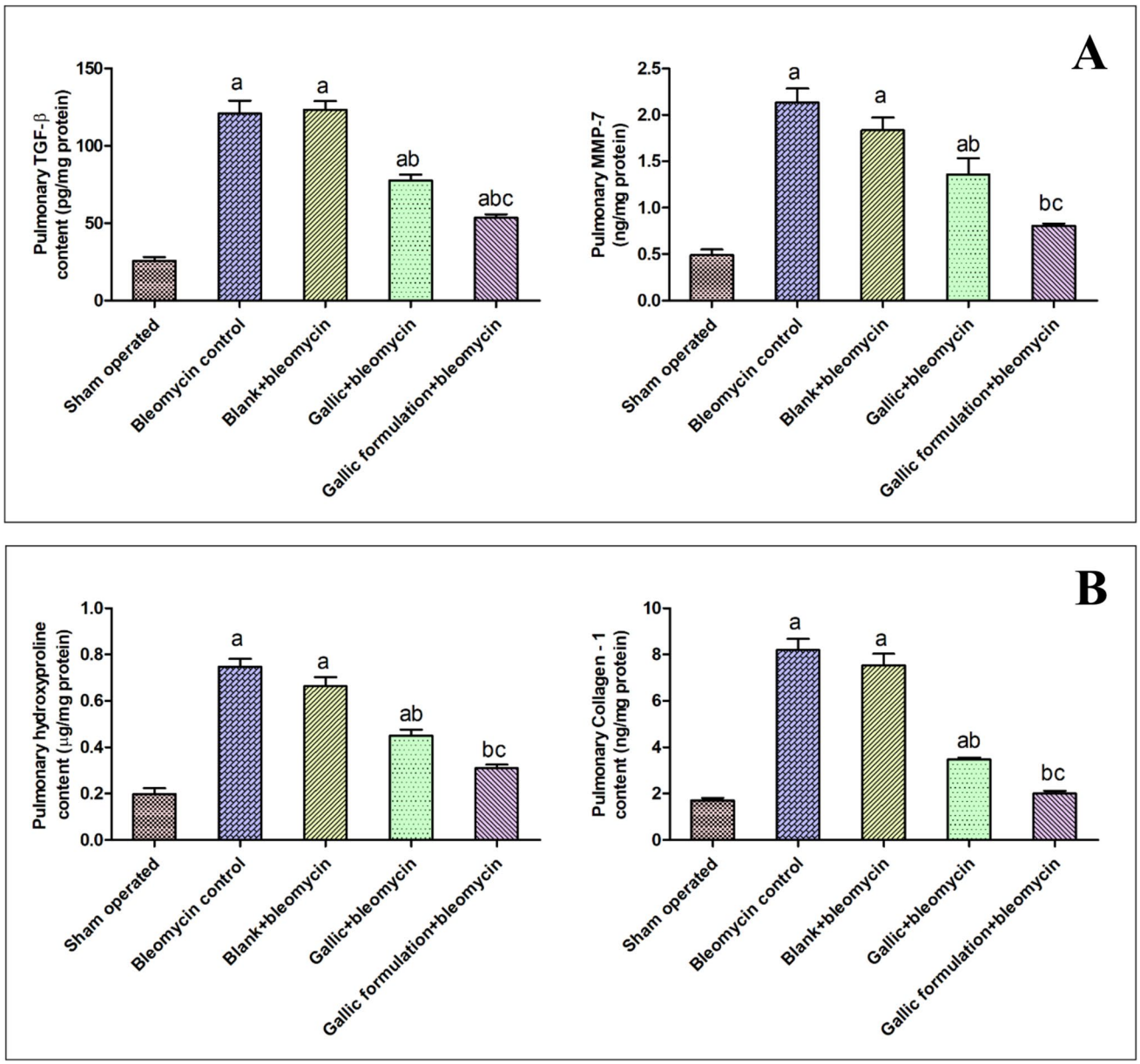

Fig. 5 **A** Effect on pulmonary levels of TGF-β and MMP-7 **B** Effect on pulmonary expression level of hydroxyproline and collagen-1. The data is presented as mean ± SEM ($n = 6$); a: significant difference from the sham operated group, b: significant difference from bleomycin control group and blank + bleomycin group, c: significant difference from gallic + bleomycin group (at $p < 0.05$)

control group (Fig. 6B) demonstrated pronounced interstitial collagen accumulation, characterized by intense blue staining, substantial thickening of alveolar septa, and distortion of parenchymal structure hallmarks of advanced pulmonary fibrosis.

Rats treated with the non-medicated formulation (Fig. 6C) showed comparable fibrotic pathology to bleomycin-control group. Notably, administration of gallic acid in conjunction with bleomycin (Fig. 6D) resulted in a moderate attenuation of fibrosis, as evidenced by reduced collagen deposition and partial restoration of alveolar integrity. This suggests a protective role for gallic acid against bleomycin-induced pulmonary damage. Most significantly, animals treated with the optimized gallic acid formulation (Fig. 6E) demonstrated markedly improved histological outcomes, including minimal collagen accumulation and near-normal alveolar morphology. Figure 6F illustrates the quantification of collagen deposition, expressed as area percentage, across the different experimental groups in lung tissue. The histopathology findings demonstrated enhanced anti-fibrotic efficacy of the formulation, potentially attributable to improved bioavailability. Collectively, the results underscore the therapeutic potential

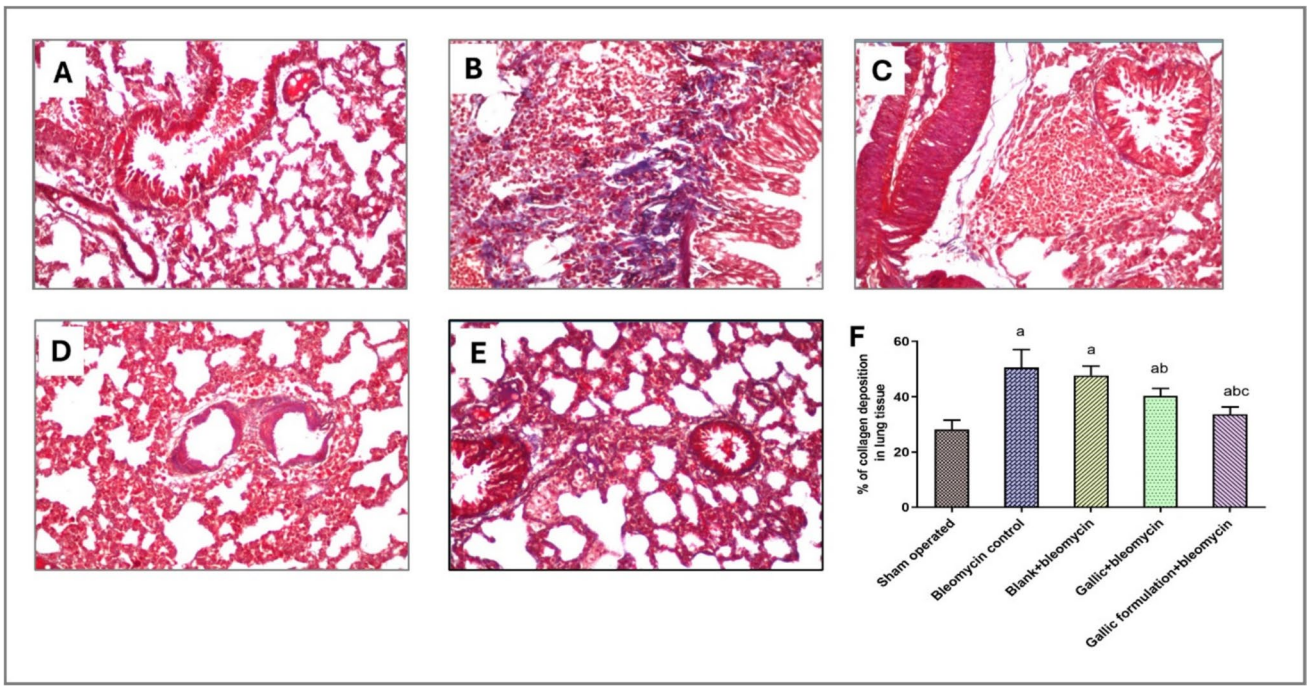

Fig. 6 Histopathological Evaluation of lung tissue using Masson Trichrome staining; **A** Sham-operated group, **B** Bleomycin-control group, **C** Plain formulation treated group, **D** Gallic acid treated group, **E** Gallic acid formulation treated group. **F** Quantification of collagen deposition across the different experimental groups in lung tissue expressed as area percentage using ImageJ software

of gallic acid, particularly in its optimized delivery form, as a promising candidate for intervention in drug-induced pulmonary fibrosis.

Conclusion

This research highlights the considerable promise of lecithin-polymer hybrid micelles in delivering gallic acid, improving its bioavailability and therapeutic effectiveness, particularly for treating pulmonary fibrosis. The optimized formula exhibited a high drug entrapment efficiency ($96.78 \pm 1.45\%$), a desirable particle size (120.22 ± 1.45 nm) for prolonged circulation by evading the reticuloendothelial system (RES), and a suitable zeta potential (-32.12 ± 0.97 mV) for stability. In contrast to the standard drug, the optimized formula showed a sustained drug release profile. *In-vivo* pharmacokinetics showed a relative bioavailability of 735% indicating greatly increased drug absorption and prolonged systemic exposure. Moreover, the optimized formula demonstrated promising results in a rat model of pulmonary fibrosis, showing significant improvements in key biomarkers such as transforming growth factor beta (TGF-ß), matrix metalloproteinase-7 (MMP-7), hydroxyproline, and collagen-1 levels. These findings highlight lecithin-polymer hybrid micelles as a promising nanocarrier system to overcome the inherent bioavailability limitations of gallic acid and potentially other drugs with similar challenges.

Future studies should prioritize evaluating the long-term stability of the system at room temperature, along with conducting comprehensive preclinical and clinical assessments to determine its safety and efficacy across diverse patient populations and to broaden its therapeutic applications.

Supplementary Information The online version contains supplementary material available at https://doi.org/10.1208/s12249-026-03351-4.

Acknowledgements The authors are deeply grateful to Dr. Christine Maged for her technical expertise and assistance in the revision and refinement of the HPLC methodology applied in this research.

Authors' Contribution Every author contributed to the design and idea of the study. Nabila M. Sweed, Mahitab H. Elbishbishy, and Mai A. Zaafan prepared the materials, collected the data, and conducted the analysis. Nabila M. Sweed wrote the initial draft of the manuscript, and other contributors praised earlier iterations. The final text was reviewed and approved by all authors.

Funding Open access funding provided by The Science, Technology & Innovation Funding Authority (STDF) in cooperation with The Egyptian Knowledge Bank (EKB).

Data Availability The corresponding author, Nabila M. Sweed, can provide the datasets created and/or analysed during the current work upon reasonable request.

Declarations

Ethics Approval The October University for Modern Sciences and Arts (MSA) faculty of Pharmacy's ethics committee authorized all techniques used in the performed animal experiments adhering to the ARRIVE criteria for laboratory animal usage (Approval number: PH77/REC77/2025PD).

Consent to Participate This study does not comprise any human subjects.

Consent for Publication This study does not comprise any human subjects.

Competing interests There are no pertinent financial or non-financial interests that the authors would want to declare.

References

1. Martinez FJ, Collard HR, Pardo A, Raghu G, Richeldi L, Selman M, et al. Idiopathic pulmonary fibrosis. Nat Rev Dis Primers. 2017;3:1–20. https://doi.org/10.1038/nrdp.2017.74.
2. Barratt SL, Creamer A, Hayton C, Chaudhuri N. Idiopathic pulmonary fibrosis (IPF): an overview. J Clin Med. 2018;7:1–21.
3. Zhang Y, Kaminski N. Biomarkers in idiopathic pulmonary fibrosis. Curr Opin Pulm Med. 2012;18:441–6.
4. King CS, Nathan SD. Practical considerations in the pharmacologic treatment of idiopathic pulmonary fibrosis. Curr Opin Pulm Med. 2015;21:479–89.
5. Xiong D, Gao F, Shao J, Pan Y, Wang S, Wei D, et al. Arctiin-encapsulated DSPE-PEG bubble-like nanoparticles inhibit alveolar epithelial type 2 cell senescence to alleviate pulmonary fibrosis via the p38/p53/p21 pathway. Front Pharmacol. 2023;14:1–19.
6. Kliment CR, Oury TD. Oxidative stress, extracellular matrix targets, and idiopathic pulmonary fibrosis. Free Radic Biol Med. 2010;49:707–17. https://doi.org/10.1016/j.freeradbiomed.2010.04.036.
7. Bocchino M, Agnese S, Fagone E, Svegliati S, Grieco D, Vancheri C, et al. Reactive oxygen species are required for maintenance and differentiation of primary lung fibroblasts in idiopathic pulmonary fibrosis. PLoS ONE. 2010. https://doi.org/10.1371/journal.pone.0014003.
8. Yang W, Yuan H, Sun H, Hu T, Xu Y, Qiu Y, et al. Co-Mn complex oxide nanoparticles as potential reactive oxygen species scavenging agents for pulmonary fibrosis treatment. Molecules. 2024. https://doi.org/10.3390/molecules29215106.
9. Dimitrios B. Sources of natural phenolic antioxidants. Trends Food Sci Technol. 2006;17:505–12.
10. Mehrzadi S, Hosseini P, Mehrabani M, Siahpoosh A, Goudarzi M, Khalili H, et al. Attenuation of bleomycin-induced pulmonary fibrosis in Wistar rats by combination treatment of two natural phenolic compounds: quercetin and gallic acid. Nutr Cancer. 2021;73:2039–49. https://doi.org/10.1080/01635581.2020.1820053.
11. Bischoff SC. Quercetin: potentials in the prevention and therapy of disease. Curr Opin Clin Nutr Metab Care. 2008;11:733–40.
12. Badhani B, Sharma N, Kakkar R. Gallic acid: a versatile antioxidant with promising therapeutic and industrial applications. RSC Adv. 2015;5:27540–57. https://doi.org/10.1039/C5RA01911G.
13. Nagpal, K., Singh, S.K. and Mishra, D.N., 2012. Nanoparticle mediated brain targeted delivery of gallic acid: in vivo behavioral and biochemical studies for improved antioxidant and antidepressant-like activity. Drug delivery, 19(8), pp.378–391.
14. Ahmed HH, Galal AF, Shalby AB, Abd-Rabou AA, Mehaya FM. Improving anti-cancer potentiality and bioavailability of gallic acid by designing polymeric nanocomposite formulation. Asian Pac J Cancer Prev. 2018;19:3137–46.
15. Gref R, Minamitake Y, Peracchia MT, Trubetskoy V, Torchilin V, Langer R. Biodegradable long-circulating polymeric nanospheres. Science. 1994;263:1600–3.
16. Kulthe SS, Choudhari YM, Inamdar NN, Mourya V. Polymeric micelles: authoritative aspects for drug delivery. Des Monomers Polym. 2012;15:465–521.
17. Osada K, Christie RJ, Kataoka K. Polymeric micelles from poly (ethylene glycol)–poly (amino acid) block copolymer for drug and gene delivery. J Royal Soc Interface. 2009;6(suppl_3):S325-39.
18. Ahmad Z, Shah A, Siddiq M, Kraatz HB. Polymeric micelles as drug delivery vehicles. RSC Adv. 2014;4:17028–38.
19. Song T, Wang H, Liu Y, Cai R, Yang D, Xiong Y. Tpgs-modified long-circulating liposomes loading ziyuglycoside i for enhanced therapy of myelosuppression. Int J Nanomedicine. 2021;16:6281–95.
20. Tan S, Zou C, Zhang W, Yin M, Gao X, Tang Q. Recent developments ind-a-tocopheryl polyethylene glycol-succinate-based nanomedicine for cancer therapy. Drug Deliv. 2017;24:1831–42. https://doi.org/10.1080/10717544.2017.1406561.
21. Mi Y, Zhao J, Feng SS. Vitamin e TPGS prodrug micelles for hydrophilic drug delivery with neuroprotective effects. Int J Pharm. 2012;438:98–106.
22. Zhang Z, Tan S, Feng SS. Vitamin E TPGS as a molecular biomaterial for drug delivery. Biomaterials. 2012;33:4889–906. https://doi.org/10.1016/j.biomaterials.2012.03.046.
23. Javed I, Hussain SZ, Ullah I, Khan I, Ateeq M, Shahnaz G, et al. Synthesis, characterization and evaluation of lecithin-based nanocarriers for the enhanced pharmacological and oral pharmacokinetic profile of amphotericin B. J Mater Chem B. 2015;3:8359–65.
24. Chen LC, Chen YC, Su CY, Wong WP, Sheu MT, Ho HO. Development and characterization of lecithin-based self-assembling mixed polymeric micellar (saMPMs) drug delivery systems for curcumin. Sci Rep. 2016;6:1–12.
25. Chen LC, Chen YC, Su CY, Hong CS, Ho HO, Sheu MT. Development and characterization of self-assembling lecithin-based mixed polymeric micelles containing quercetin in cancer treatment and an in vivo pharmacokinetic study. Int J Nanomedicine. 2016;11:1557–66.
26. Yue PF, Zheng Q, Wu B, Yang M, Wang MS, Zhang HY, et al. Process optimization by response surface design and characterization study on geniposide pharmacosomes. Pharm Dev Technol. 2012;17:94–102.
27. Sweed NM, Dawoud MHS, Aborehab NM, Ezzat SM. An approach for an enhanced anticancer activity of ferulic acid-loaded

polymeric micelles via MicroRNA-221 mediated activation of TP53INP1 in caco-2 cell line. Sci Rep. 2024. https://doi.org/10.1038/s41598-024-52143-y.
28. Dawoud MHS, Fayez AM, Mohamed RA, Sweed NM. Optimization of nanovesicular carriers of a poorly soluble drug using factorial design methodology and artificial neural network by applying quality by design approach. Pharm Dev Technol. 2021;26:1035–50. https://doi.org/10.1080/10837450.2021.1980009.
29. Sweed NM, Zaafan MA, El-Bishbishy MH, Dawoud MH. The pulmonary protective potential of vanillic acid-loaded TPGS-liposomes : modulation of miR-217 / MAPK / NF- κ b signalling pathway. J.Microencapsul [Internet]. 2024;41:255–68. https://doi.org/10.1080/02652048.2024.2335166.
30. Sweed NM, Fayez AM, El-Emam SZ, Dawoud MHS. Response surface optimization of self nano-emulsifying drug delivery system of rosuvastatin calcium for hepatocellular carcinoma. J Pharm Investig. 2021;51:85–101. https://doi.org/10.1007/s40005-020-00497-6.
31. Russo A, Pellosi DS, Pagliara V, Milone MR, Pucci B, Caetano W, et al. Biotin-targeted Pluronic® P123/F127 mixed micelles delivering niclosamide: a repositioning strategy to treat drug-resistant lung cancer cells. Int J Pharm. 2016;511:127–39. https://doi.org/10.1016/j.ijpharm.2016.06.118.
32. Radwan SAA, El-Maadawy WH, ElMeshad AN, Shoukri RA, Yousry C. Correction to: impact of reverse micelle loaded lipid nanocapsules on the delivery of gallic acid into activated hepatic stellate cells: a promising therapeutic approach for hepatic fibrosis. Pharm Res. 2020;37. https://doi.org/10.1007/s11095-020-02891.
33. Vrignaud S, Anton N, Gayet P, Benoit JP, Saulnier P. Reverse micelle-loaded lipid nanocarriers: a novel drug delivery system for the sustained release of doxorubicin hydrochloride. Eur J Pharm Biopharm. 2011;79:197–204. https://doi.org/10.1016/j.ejpb.2011.02.015.
34. Pavaloiu RD, Sha'at F, Hlevca C, Sha'at M, Savoiu G, Osman S. Evaluation of drug release kinetics from polymeric nanoparticles loaded with poorly water-soluble APIs. In vivo. 2021;1:2.
35. Uchegbu IF, Breznikar J, Zaffalon A, Odunze U, Schätzlein AG. Polymeric micelles for the enhanced deposition of hydrophobic drugs into ocular tissues, without plasma exposure. Pharmaceutics. 2021. https://doi.org/10.3390/pharmaceutics13050744.
36. El-zaafarany GM, Soliman ME, Mansour S, Awad GAS. Identifying lipidic emulsomes for improved oxcarbazepine brain targeting : in vitro and rat in vivo studies. Int J Pharm. 2016;503:127–40. https://doi.org/10.1016/j.ijpharm.2016.02.038.
37. Jadhav P, Bothiraja C, Pawar A. Resveratrol-piperine loaded mixed micelles: formulation, characterization, bioavailability, safety and in vitro anticancer activity. RSC Adv. 2016;6:112795–805.
38. Ma F, Gong X, Zhou X, Zhao Y, Li M. An UHPLC-MS/MS method for simultaneous quantification of gallic acid and protocatechuic acid in rat plasma after oral administration of Polygonum capitatum extract and its application to pharmacokinetics. J Ethnopharmacol. 2015;162:377–83. https://doi.org/10.1016/j.jep.2014.12.044.
39. Zaafan MA, Haridy AR, Abdelhamid AM. Amitriptyline attenuates bleomycin-induced pulmonary fibrosis: modulation of the expression of NF-κβ, iNOS, and Nrf2. Naunyn Schmiedebergs Arch Pharmacol. 2019;392:279–86.
40. Zaafan MA, Zaki HF, El-Brairy AI, Kenawy SA. Pyrrolidinedithiocarbamate attenuates bleomycin-induced pulmonary fibrosis in rats: modulation of oxidative stress, fibrosis, and inflammatory parameters. Exp Lung Res. 2016;42:408–16. https://doi.org/10.1080/01902148.2016.1244578.
41. Li TP, Wong WP, Chen LC, Su CY, Chen LG, Liu DZ, et al. Physical and Pharmacokinetic Characterizations of trans-Resveratrol (t-Rev) Encapsulated with Self-Assembling Lecithin-based Mixed Polymeric Micelles (saLMPMs). Sci Rep [Internet]. 2017;7:1–10. https://doi.org/10.1038/s41598-017-11320-y.
42. Tănase MA, Soare AC, Diţu LM, Nistor CL, Mihaescu CI, Gifu IC, et al. Influence of the hydrophobicity of Pluronic micelles encapsulating curcumin on the membrane permeability and enhancement of photoinduced antibacterial activity. Pharmaceutics. 2022. https://doi.org/10.3390/pharmaceutics14102137.
43. Luo H, Jiang K, Liang X, Liu H, Li Y. Small molecule-mediated self-assembly behaviors of Pluronic block copolymers in aqueous solution: impact of hydrogen bonding on the morphological transition of Pluronic micelles. Soft Matter. 2019;16:142–51.
44. Wu Y, Chu Q, Tan S, Zhuang X, Bao Y, Wu T, et al. D-α-tocopherol polyethylene glycol succinate-based derivative nanoparticles as a novel carrier for paclitaxel delivery. Int J Nanomedicine. 2015;10:5219–35.
45. Chang CE, Hsieh CM, Huang SC, Su CY, Sheu MT, Ho HO. Lecithin-stabilized polymeric micelles (LsbPMs) for delivering quercetin: pharmacokinetic studies and therapeutic effects of quercetin alone and in combination with doxorubicin. Sci Rep. 2018;8:1–11.
46. Holm R, Jensen IHM, Sonnergaard J. Optimization of self-microemulsifying drug delivery systems (SMEDDS) using a D-optimal design and the desirability function. Drug Dev Ind Pharm. 2006;32:1025–32.
47. Dawoud MHS, Abdel-Daim A, Nour MS, Sweed NM. A quality by design paradigm for albumin-based nanoparticles: formulation optimization and enhancement of the antitumor activity. J Pharm Innov. 2023;18:1395–414. https://doi.org/10.1007/s12247-022-09698-y.
48. Isailović T, Dordević S, Marković B, Randelovic D, Cekić N, Lukić M, et al. Biocompatible Nanoemulsions for Improved Aceclofenac Skin Delivery: Formulation Approach Using Combined Mixture-Process Experimental Design. J Pharm Sci. 2016;105:308–23.
49. Sweed NM, Elbalkiny HT, Magdy E, Ramadan M, Mahmoud S, Mohamed T, et al. Optimization of Linagliptin-loaded polymersomes via response surface methodology: a repurposed therapeutic strategy for hepatic encephalopathy prevention. J Drug Deliv Sci Technol. 2025;108:106855. https://doi.org/10.1016/j.jddst.2025.106855.
50. Wianowska D, Olszowy-Tomczyk M. A concise profile of gallic acid—from its natural sources through biological properties and chemical methods of determination. Molecules. 2023. https://doi.org/10.3390/molecules28031186.
51. Dutra LMU, Ribeiro MENP, Cavalcante IM, De Brito DHA, De Moraes SL, Da Silva RF, et al. Binary mixture micellar systems of F127 and P123 for griseofulvin solubilisation. Polimeros. 2015;25:433–9.
52. Osouli M, Abdollahizad E, Alavi S, Mahboubi A, Abbasian Z, Haeri A, et al. Biocompatible phospholipid-based mixed micelles for posaconazole ocular delivery: Development, characterization, and in - vitro antifungal activity. J Biomater Appl. 2023;37:969–78.
53. Xu W, Ling P, Zhang T. Polymeric micelles, a promising drug delivery system to enhance bioavailability of poorly water-soluble drugs. J Drug Deliv. 2013;2013:1–15.
54. Li H, Yan L, Tang EKY, Zhang Z, Chen W, Liu G, et al. Synthesis of TPGS/curcumin nanoparticles by thin-film hydration and evaluation of their anti-colon cancer efficacy in vitro and in vivo. Front Pharmacol. 2019;10:1–12.
55. Mod Razif MRF, Chan SY, Widodo RT, Chew YL, Hassan M, Hisham SA, et al. Optimization of a Luteolin-Loaded TPGS/Poloxamer 407 nanomicelle: the effects of copolymers, hydration temperature and duration, and freezing temperature on encapsulation efficiency, particle size, and solubility. Cancers. 2023. https://doi.org/10.3390/cancers15143741.

56. Butt AM, Amin MCIM, Katas H, Sarisuta N, Witoonsaridsilp W, Benjakul R. In vitro characterization of pluronic F127 and D-α-tocopheryl polyethylene glycol 1000 succinate mixed micelles as nanocarriers for targeted anticancer-drug delivery. J Nanomater. 2012. https://doi.org/10.1155/2012/916573.
57. Zhao X, Liu J, Hu Y, Fan Y, Wang D, Yuan J, et al. Optimization on condition of glycyrrhetinic acid liposome by rsm and the research of its immunological activity. Int J Biol Macromol. 2012;51:299–304. https://doi.org/10.1016/j.ijbiomac.2012.05.005.
58. Dawoud MHS, Zaafan MA, Saleh SS, Mannaa IM, Sweed NM. Response surface optimization of a cardioprotective compound through pharmacosomal drug delivery system: in vivo bioavailability and cardioprotective activity potential. Drug Deliv Transl Res. 2023;13:2315–39. https://doi.org/10.1007/s13346-023-01315-w.
59. Elsharkawy FM, Amin MM, Shamsel-Din HA, Ibrahim W, Ibrahim AB, Sayed S. Self-assembling lecithin-based mixed polymeric micelles for nose to brain delivery of clozapine: In-vivo assessment of drug efficacy via radiobiological evaluation. Int J Nanomedicine. 2023;18:1577–95.
60. Bao R, Wang QL, Li R, Adu-Frimpong M, Toreniyazov E, Ji H, et al. Improved oral bioavailability and target delivery of 6-shogaol via vitamin E TPGS-modified liposomes: preparation, in-vitro and in-vivo characterizations. J Drug Deliv Sci Technol. 2020;59:101842. https://doi.org/10.1016/j.jddst.2020.101842.
61. Ebrahimi HA, Javadzadeh Y, Hamidi M, Jalali MB. Repaglinide-loaded solid lipid nanoparticles: effect of using different surfactants/stabilizers on physicochemical properties of nanoparticles. DARU J Pharm Sci. 2015;23:1–11. https://doi.org/10.1186/s40199-015-0128-3.
62. Wu YZ, Tsai YY, Chang LS, Chen YJ. Evaluation of gallic acid-coated gold nanoparticles as an anti-aging ingredient. Pharmaceuticals. 2021. https://doi.org/10.3390/ph14111071.
63. Butt AM, Iqbal MC, Amin M, Katas H. Synergistic effect of pH-responsive folate-functionalized poloxamer 407-TPGS-mixed micelles on targeted delivery of anticancer drugs. Int J Nanomedicine. 2015;10:1321–34. https://doi.org/10.2147/IJN.S78438.
64. Sun C, Li W, Ma P, Li Y, Zhu Y, Zhang H, et al. Development of TPGS/F127/F68 mixed polymeric micelles: enhanced oral bioavailability and hepatoprotection of syringic acid against carbon tetrachloride-induced hepatotoxicity. Food Chem Toxicol. 2020;137: 111126. https://doi.org/10.1016/j.fct.2020.111126.
65. Cerqueira R, Domingues C, Veiga F, Jarak I, Figueiras A. Development and characterization of curcumin-loaded TPGS/F127/P123 polymeric micelles as a potential therapy for colorectal cancer. Int J Mol Sci. 2024;25:1–22.
66. Papadopoulou V, Kosmidis K, Vlachou M, Macheras P. On the use of the Weibull function for the discernment of drug release mechanisms. Int J Pharm. 2006;309:44–50.
67. Patra A, Satpathy S, Shenoy AK, Bush JA, Kazi M, Hussain MD. Formulation and evaluation of mixed polymeric micelles of quercetin for treatment of breast, ovarian, and multidrug resistant cancers. Int J Nanomedicine. 2018;13:2869–81.
68. Telange DR, Patil AT, Pethe AM, Fegade H, Anand S, Dave VS. Formulation and characterization of an apigenin-phospholipid phytosome (APLC) for improved solubility, in vivo bioavailability, and antioxidant potential. Eur J Pharm Sci. 2017;108:36–49.
69. Kanade R, Boche M, Pokharkar V. Self-assembling raloxifene loaded mixed micelles: formulation optimization, in vitro cytotoxicity and in vivo pharmacokinetics. AAPS PharmSciTech. 2018;19:1105–15.
70. Nanri Y, Nunomura S, Terasaki Y, Yoshihara T, Hirano Y, Yokosaki Y, et al. Cross-talk between transforming growth factor-b and periostin can be targeted for pulmonary fibrosis. Am J Respir Cell Mol Biol. 2020;62:204–16.
71. Dogu Zengin D, Ergun D, Yormaz B, Ergun R, Guven H, Korez MK, et al. The role of serum prolidase activity, MMP-1, MMP-7, and TGF-β values in the prediction of early fibrosis in patients with moderate to severe COVID-19. Viruses. 2025;17:1–17.
72. Nikbakht J, Hemmati AA, Arzi A, Mansouri MT, Rezaie A, Ghafourian M. Protective effect of gallic acid against bleomycin-induced pulmonary fibrosis in rats. Pharmacol Rep. 2015;67:1061–7. https://doi.org/10.1016/j.pharep.2015.03.012.
73. Rong Y, Cao B, Liu B, Li W, Chen Y, Chen H, et al. A novel Gallic acid derivative attenuates BLM-induced pulmonary fibrosis in mice. Int Immunopharmacol. 2018;64:183–91. https://doi.org/10.1016/j.intimp.2018.08.024.